RANGE DOPPLER ALGORITHM OF THE MULTI-RECEIVER SAS IN THE SQUINT MODE

1st Haoran 1st Wu[a], 2nd Jinsong 2nd Tang[a], 3rd Mengbo 3nd Ma[a]

[a] Electronic College of Engineering, Naval University of Engineering

Electronic College of Engineering, Naval University of Engineering, No.717 Jiefang Road, Wuhan, People's Republic of China.
E-mail: wuhaoran_wh@163.com

Abstract: *Range Doppler Algorithm (RDA) is the most commonly used imaging algorithm for synthetic aperture radar (SAR) and synthetic aperture sonar (SAS). The multi-receiver SAS has a higher complexity than SAR, and there is little literature on multi-receiver SAS imaging algorithm in the squint mode. This paper studies RDA of the multi-receiver SAS in the squint mode.1, The "non-stop-go-stop" signal model is established for squint multi-aperture SAS. 2, A squint multi-receiver range doppler algorithm (SMRRDA) is proposed.3, The simulation experiments and the measured data show that the signal model presented in this paper is correct and SMRRDA is effective.*

Keywords: *Range Doppler Algorithm, synthetic aperture sonar, squint*

1. INTRODUCTION

Multiple receiver apertures have been suggested to overcome the inherent limitations of the synthetic aperture imaging system to achieve imaging with high resolution and a high coverage rate [1, 2]. The “stop-go-stop” hypothesis, which often used in SAS, is no longer applied in multi-receiver SAS.

In 1999 and 2002, respectively, Tang [3] and Callow [4] derived the accurate expression of the “non-stop-go-stop” time. It is a formula that shows that the “non-stop-go-stop” time is a two-dimensional variable function involving range and azimuth time. Banifant [5] expounded the approximation problem of “non-stop-go-stop” time firstly and proposed the use of delay at the center of the whole scene instead of the “non-stop-go-stop” time, but this method does not consider the spatial variability of range. Yang [6] proposed the use of time with the range variable instead of the “non-stop-go-stop” time, but this method does not consider the spatial variability of azimuth. All these methods are based on the side-looking multi-receiver SAS, but so far, no imaging algorithm for processing squint multi-receiver SAS data has been reported.

The range Doppler algorithm (RDA) was developed in 1976-1978 for processing SEASAT SAR data [7, 8]. The first digitally processed spaceborne SAR image was made with this algorithm in 1978, and it is still in wide spread use today. The algorithm is designed to achieve block processing efficiency, using frequency domain operations in both range and azimuth, while maintaining the simplicity of one-dimensional operations. It take advantage of the approximate separability of processing in these two directions, allowed by the large difference in time scales of the range and azimuth data, and by the use of range cell migration correction (RCMC) between the two one-dimensional operations. This article propose a squint multi-receiver range doppler algorithm (SMRRDA), which is used to handle data from the squint multi-receiver synthetic aperture sonar. In the following sections, SAS refers to multi-receiver SAS.

This article is organized as follows. Section 2 presents the model of the accurate instantaneous slant range and signal model of a point target. Section 3 deduces the SMRRDA . In Section 4, some simulations are performed to verify the proposed algorithm. In Section 5, some comments are given.

2. MODELING THE SQUINT SAS

In this section, we evaluate the model of the accurate instantaneous slant range for squint SAS based on a general squint multi-receiver geometry, as shown in Fig. 1.

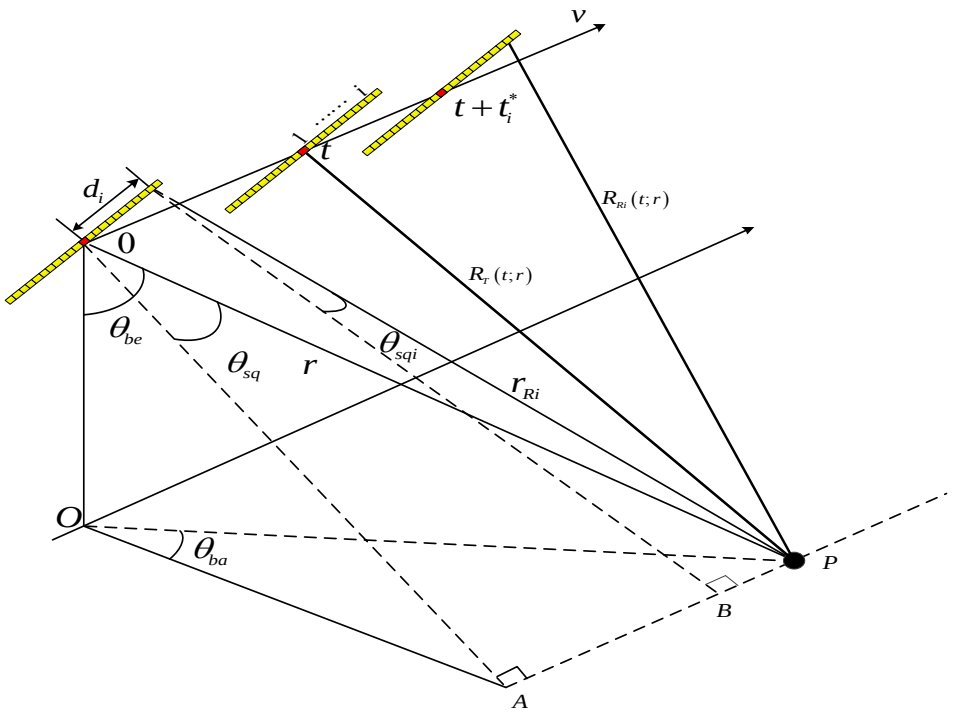

Fig.1: Geometry model of the squint SAS.

The symbols in Fig. 1 and their definitions are given as follows.

- v : Platform velocity,
- d_i : The baseline between the transmitter and the i th receiver,
- O : The starting point of the slow time,
- P : The point target,
- θ_{ba} : The yaw angle,
- θ_{be} : The look-down angle,
- r : The slant range between the transmitter and the point target at the beam center crossing time,
- r_{Ri} : The slant range between the i th receiver and the point target at the beam center crossing time,
- θ_{sq} : The squint angle of the transmitter at the beam center crossing time,
- θ_{sqi} : he squint angle of the i th receiver at the beam center crossing time,
- t : The slow time,
- t_i^* : The accurate delay of the i th receiver,
- $R_T(t;r)$: The instantaneous slant range from the point target to the transmitter,
- $R_{Ri}(t;r)$: The instantaneous slant range from the point target to the i th receiver,
- ■: Transmit-receive sharing antenna,
- □: Receive aperture antenna.

.. According to the geometry model in Fig. 1, the accurate instantaneous slant range to the point target (P) is given by.

$$\begin{aligned} R_i^*(t;r) &= R_T(t;r) + R_{Ri}(t;r) \\ &= \sqrt{r^2 + v^2t^2 - 2vtr\sin\theta_{sq}} \\ &+ \sqrt{r_{Ri}^2 + v^2\left(t + t_i^*\right)^2 - 2v\left(t + t_i^*\right)r_{Ri}\sin\theta_{sqi}} \end{aligned} \tag{1}$$

where $\sin\theta_{sqi}$ is $\left(r\sin\theta_{sq} - d_i\cos\theta_{ba}\right)/r_{Ri}$, r_{Ri} represents $\sqrt{r^2 + d_i^2}$, and t_i^* is the "non-stop-go-stop" time and expressed by (2), which is shown at the bottom of the page. Considering the complexity of (2), t_i^* is approximated as $2r/c$.

$$\begin{aligned} t_i^* = &\frac{tv^2 - vr_{Ri}\sin\theta_{sqi} + c\sqrt{r^2 + v^2t^2 - 2vtr\sin\theta_{sq}}}{c^2 - v^2} \\ &+ \frac{\sqrt{\left(tv^2 - vr_{Ri}\sin\theta_{sqi} + c\sqrt{r^2 + v^2t^2 - 2vtr\sin\theta_{sq}}\right)^2 + \left(c^2 - v^2\right)\left(2vtd_i\cos\theta_{ba} + d_i^2\right)}}{c^2 - v^2} \end{aligned} \tag{2}$$

Because two square root terms are included in (1), the analytical point of stationary phase t cannot be obtained easily. To circumvent this limitation, $R_i^*(t;r)$ is approximated as follows:

$$R_i(t;r) \approx R_T\left(t + \frac{r}{c} + \frac{d_i\cos\theta_{ba}}{2v};r\right) + \Delta R\left(r;d_i\right) \tag{3}$$

$$\Delta R\left(r;d_i\right) = r + \sqrt{r_{Ri}{}^2 + 4r^2v^2/c^2 - 4vrr_{Ri}\sin\theta_{sqi}/c} - 2\sqrt{r^2\cos^2\theta_{sq} + v^2\left(t_i - r\sin\theta_{sq}/v\right)^2} \tag{4}$$

The phase error, which is caused by the approximation of $R_i^*(t;r)$, is given by

$$\sigma = 2\pi\left(\frac{R_i(t;r) - R_i^*(t;r)}{\lambda}\right) \tag{5}$$

The simulation result of σ is shown in Fig. 2. The simulation parameters are $\lambda = 0.02m$, $v = 3\,m/s$, $d_i = 3m$, and $\theta_{sq} = 2^0$.

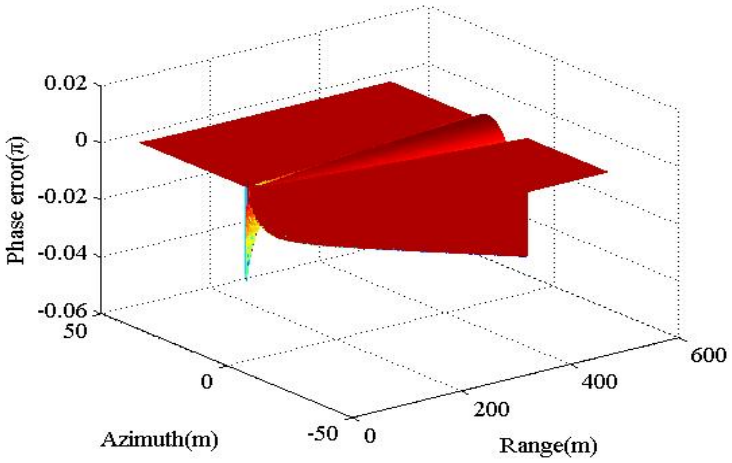

Fig.2. Phase error.

After demodulation to baseband, the received signal of the i th receiver comes from the point target (P) (as shown in Fig. 1), which is approximately expressed as

$$ss_i(\tau,t;r)=p\left(\tau-\frac{R_i\ (t;r)}{c}\right)\cdot\omega_a(t)\cdot\exp\left\{j\pi k\left(\tau-\frac{R_i\ (t;r)}{c}\right)^2\right\}\cdot\exp\left\{-j\frac{2\pi f_0}{c}R_i\ (t;r)\right\} \tag{6}$$

where τ is the fast time, $p(.)$ is the pulse envelope, $\omega_a(.)$ is the antenna weighting, k is the FM rate, c is the speed of sound, and f_0 is the carrier frequency.

3. THE DERIVATION OF SMRRDA

The SMRRDA proposed in this paper is used to focus the squint multi-receiver SAS data, and is shown in the thick-lined boxes in Fig.3.

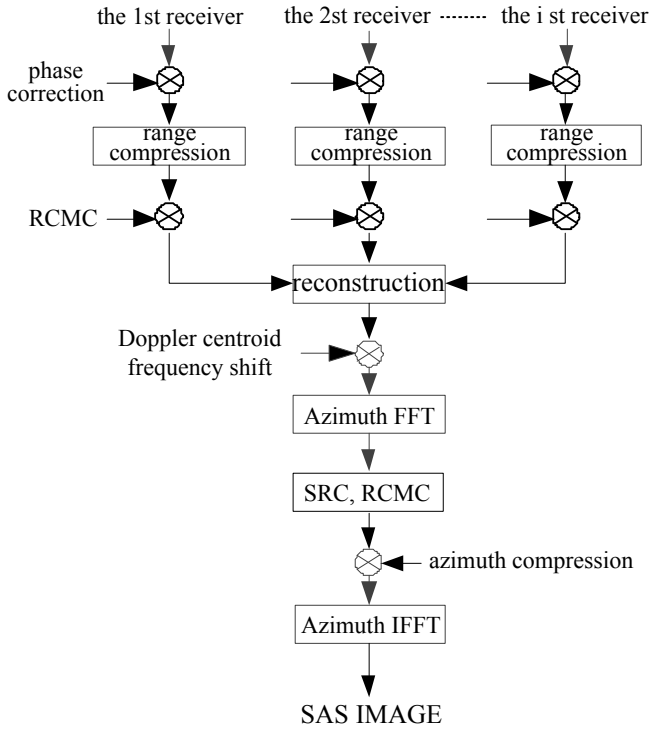

Fig.3. Functional block diagram of the SMRRDA.

A. Multi-receiver data processing

The phase correction is based on an analysis of the multi-receiver signal's phase compared to the phase of a monostatic and uniformly-sampled signal. The phase correction function is given by

$$\phi_i = e\,\mathrm{xp}\left\{ j\frac{2\pi f_0}{c}\Delta R\left(r;d_i\right)\right\} \tag{7}$$

The range cell migration corresponding to $\Delta R\left(r;d_i\right)/c$ is greatly affected by the range and squint angle, which is proportional to the range and inversely proportional to the angle. This range migration cannot be ignored. Here, phase multiplication is used in the range frequency domain to correct this term on the reference range. The range cell migration correction (RCMC) function is given by

$$\psi_i\left(f_r\right) = e\,\mathrm{xp}\left\{ j\frac{2\pi f_r}{c}\Delta R\left(r_{ref};d_i\right)\right\} \tag{8}$$

where f_r represents the range frequency, and r_{ref} represents the reference range. After the phase correction and RCMC, the signal is given by

$$Ss_i(f_r,t;r)=W_r(f_r)\omega_a(t)\cdot\exp\left\{-j\frac{\pi f_r^2}{k}\right\}\cdot\exp\left\{-j\frac{2\pi(f_0+f_r)}{c}R_T(t+\frac{r}{c}+\frac{d_i\cos\theta_{ba}}{2v};r)\right\} \tag{9}$$

where $W_r(.)$ represents the range frequency envelope.

B. Reconstruction azimuth data

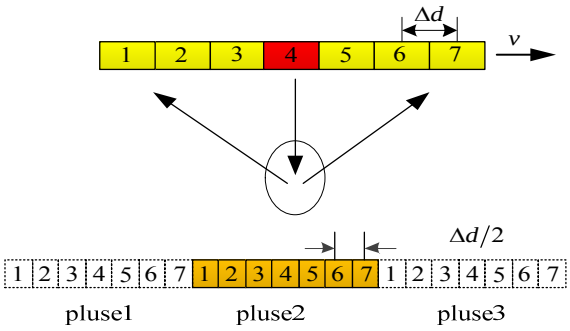

Fig.4. Displaced phase centre antenna.

After multi-receiver data processing, the instantaneous slant range can be written by

$$R_i(t;r)\approx 2\sqrt{r^2+(vt+v\frac{r}{c}+\frac{d_i}{2})^2} \tag{10}$$

The concept of Displaced Phase Centre Antenna (DPCA) is introduced to multi-receiver side-looking SAR [1]. Assume the size of sub-receiver $\Delta d=d_{i+1}-d_i$, and the platform velocity v are fixed, the multi-receiver SAS/SAR can be taken to be a single receiver SAS/SAR, which has a specific *PRF* to fulfill the timing constraint for uniform sampling.

$$PRF=\frac{2v}{I\Delta d} \tag{11}$$

where I is the number of receivers as shown in Fig.4. For the nonuniform DPCA sampling case, the reference [2] provides a solution. After DPCA sampling, the azimuth data can be obtained by (12) and the sampling frequency is $2v/\Delta d$.

$$ss(\tau,t;r)=p\left(\tau-\frac{R(t;r)}{c}\right)\cdot\omega_a(t)\cdot\exp\left\{j\pi k\left(\tau-\frac{R(t;r)}{c}\right)^2\right\}\cdot\exp\left\{-j\frac{2\pi f_0}{c}R(t;r)\right\} \tag{12}$$

Where

$$R(t;r) = 2\sqrt{r^2 + (vt + v\frac{r}{c})^2} \tag{13}$$

C. Doppler centroid frequency shift

In the squint condition, the signal energy is wraparound in the azimuth frequency domain [9]. The problem can be resolved by multiplying the linear phase $\exp(-j2\pi f_{dc}t)$, According to (1) , the Doppler centroid frequency f_{dc} is given by

$$f_{dc} = -\frac{1}{\lambda}\frac{dR_i(t;r)}{dt}\bigg|_{t=0} = \frac{v\sin(\theta_{sq})}{\lambda} + \frac{v\sin(\theta_{sqi})}{\lambda} \tag{14}$$

In(14), λ is the wavelength. In general case, r is much longer than d_i , so f_{dc} can be approximated by $2v\sin(\theta_{sq})/\lambda$.

D. Range Cell Migration Correction

This signal is transformed into the 2-D frequency domain by applying the principle of stationary in the azimuth time domain. Then the signal is given by

$$SS(f_r, f_a; r) = W_r(f_r)W_a(f_a)\exp\{j\theta(f_r, f_a; r)\} \tag{15}$$

where $W_a(\bullet)$ represents the azimuth frequency envelope, f_a represents the azimuth frequency, $\theta(f_r, f_a; r)$ represents the phase of $S(f_r, f_a; r)$ .To facilitate the development of processing algorithm, we expand $\theta(f_r, f_a; r)$ around f_r . The expanded series are truncated at the second-order term and expressed as follows:

$$\theta(f_r, f_a; r) = -\frac{4\pi r\cos(\theta_{sq})f_0}{c}D(f_a) + 2\pi\Delta t f_a - 2\pi\frac{2r\cos(\theta_{sq})}{cD(f_a)}f_r - \frac{\pi}{k_s}f_r^2 \tag{16}$$

where Δt is $r/c - r\sin(\theta_{sq})/v + N\Delta d\cos(\theta_{ba})/2v$, $D(f_a)$ is the migration factor, and $k_s(f_a; r)$ is the range-frequency rate. They are given as follows：

$$\theta(f_r, f_a; r) = -\frac{4\pi r\cos(\theta_{sq})f_0}{c}D(f_a) + 2\pi\Delta t f_a - 2\pi\frac{2r\cos(\theta_{sq})}{cD(f_a)}f_r - \frac{\pi}{k_s}f_r^2 \tag{17}$$

Where

$$D(f_a)=\sqrt{1-\frac{c^2 f_a^2}{4v^2 f_0^2}} \tag{18}$$

$$\frac{1}{k_s(f_a;r)}=\frac{2r\cos(\theta_{sq})}{cf_0}\left(\frac{1}{D}-\frac{1}{D^3}\right)+\frac{1}{k} \tag{19}$$

The range inverse Fourier transform of(15), can be evaluated approximately by the principle of stationary phase. The range Doppler domain can then be shown to be

$$sS(\tau, f_a;r)=w_r(\tau)W_a(f_a)\exp\{j\theta(\tau, f_a;r)\} \tag{20}$$

$$\theta(\tau, f_a;r)=-\frac{4\pi r\cos(\theta_{sq})f_0}{c}D+2\pi f_a\Delta t+\pi k_s\left(\tau-\frac{2r\cos(\theta_{sq})}{c}\frac{1}{D}\right)^2 \tag{21}$$

According to (21), the amount of range cell migration to correct is given by

$$\Delta\tau=\frac{2r\cos\left(\theta_{sq}\right)}{c}\left(\frac{1}{D}-1\right) \tag{22}$$

4. SIMULATION RESULTS

To verify the validity of the squint multi-receiver RDA in the paper, simulations are carried out in this section. The system parameters are listed in Table I.

Carrier frequency	150kHz	Antenna length(transmitter)	0.08m
Bandwidth	20kHz	Antenna length(receiver)	0.08m
Pulse width	10ms	Velocity	2.5m/s
PRI	200ms	Receiver number	25
Target coordinate	(126,12)	Squint angle	$0,2^0$

Table 1: Sas System Parameters.

Fig. 5 shows the result of processing one simulated point target for different squint angles. Table II summarizes the point target analysis for cases with the different squint angles. The simulation results in Fig. 5 and Table II show that the range resolution, the azimuth resolution, the sidelobe ratio, and the target location all reach the value.

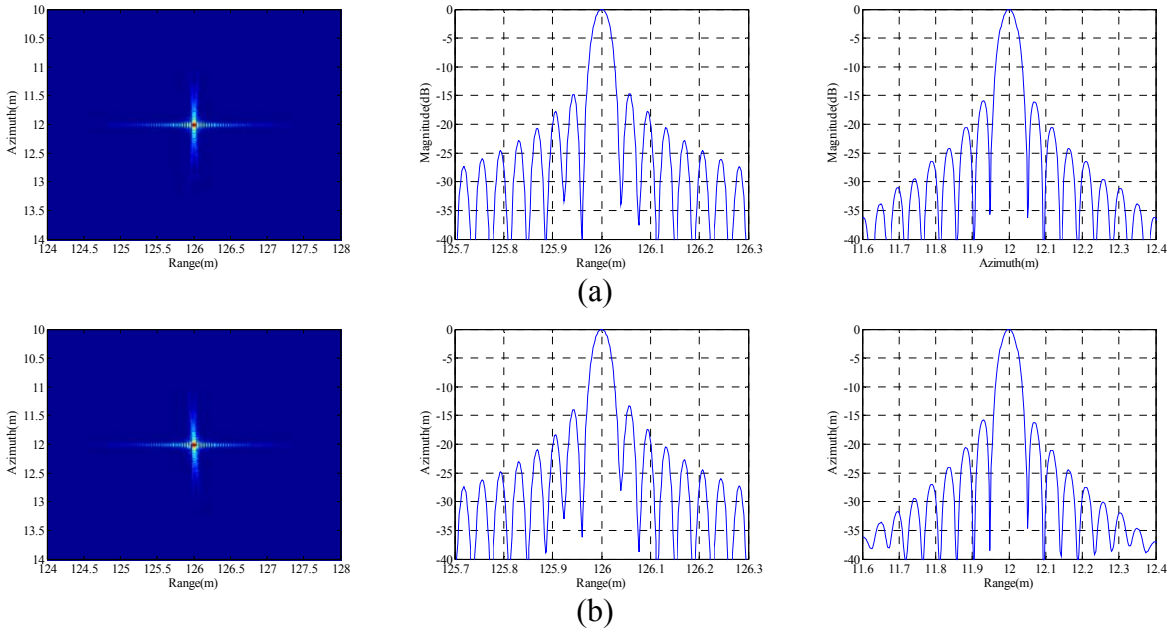

Fig. 9. Simulated SAS data processed using different squint angles. The sub-images from left to right in each row correspond to the image of point target, magnitude of range slice, and the magnitude of azimuth slice. The squint angle in (a) is 0^0, and in (b) it is 2^0.

Analyzed Parameters	Measured	
Squint angle	0^0	2^0
Range resolution	0.97 cells	1 cells
Azimuth resolution	1.1 cells	1.1 cells
Range PSLR	-14.6dB	-13.3dB
Azimuth PSLR	-15.9dB	-15.8dB

Table 2: Parameters Image Quality Parameters.

5. CONCLUSION

In this paper, the "non-stop-go-stop" signal model is established, and the SMMRDA is proposed. The key steps of SMMRDA are deduced, and the simulations show that the SMMRDA can handle SAS data with small squint angle accurately and effectively. This algorithm is conducive to the development of motion compensation for SAS and multi-receiver SAR.

6. ACKNOWLEDGEMENTS

This work was partially supported by the National Science Foundation of China (Grant no. 61671461).The authors would like to thank all anonymous reviews for the careful and detailed revision that help to improve this paper.

REFERENCES

[1] **N.Gebert, G. Krieger, A. Moreira**, SAR signal reconstruction from non-uniform displaced phase centre sampling in the presence of perturbations, In *Geoscience and Remote Sensing Symposium*, 2005.

[2] **G.A. Gilmour**, Synthetic aperture side-looking sonar system, *Journal of the Acoustical Society of America*, volume (65), pp. 557-562, 1978.

[3] **J. S. Tang, C. H. Zhang, Q. H. Li**, Research on multi-aperture synthetic aperture sonar imaging algorithm, In *1999 Chinese Academy of Sciences Institute of Acoustics Youth Academic Exchange*, Beijing, 1999.

[4] **H. J. Callow**, *Signal processing for synthetic aperture sonar image enhancement*, University of Canterbury, Christchurch, 2003.

[5] **W.J. Bonifant**, *Interferometric synthetic aperture sonar processing*, Georgia Institute of Technology, USA, 1999.

[6] **H. L. Yang**, *Studies on imaging algorithm of multiple-receiver synthetic sonar*, Naval University of Engineering, China, 2009.

[7] **C.Wu**, Processing of SEASAT SAR Data, In *SAR technology Symp*, Las Cruces,1997.

[8] **A.M.Barber**, Theory of Digital Imaging from Orbital Synthetic Aperture Radar , *International Journal of Remote Sensing*, volume (12), pp. 235-2151, 1991.

[9] **I. G. Cumming, F. H. Wong**, *Digital processing of synthetic aperture radar data*, Norwood, Artech House, pp. 236-247, 2005.